Cooperative Stabilization of a Molten Globule Apoflavodoxin Fragment†

Susana Maldonado,‡ María Ángeles Jiménez,§ Grant M. Langdon,§ and Javier Sancho*,‡

Departamento de Bioquímica y Biología Molecular y Celular, Facultad de Ciencias, Universidad de Zaragoza, 50009 Zaragoza, Spain, and Instituto de Estructura de la Materia, CSIC, 28006 Madrid, Spain

Received February 16, 1998; Revised Manuscript Received May 26, 1998

ABSTRACT: We have destabilized apoflavodoxin by site-specific excision of its C-terminal helix. The resulting flavodoxin fragment (Fld1−149) is compact and monomeric at pH 7.0, with spectroscopic properties of a molten globule and a low conformational stability. To study if Fld1−149 is cooperatively stabilized, we have measured the equilibrium urea unfolding by fluorescence, circular dichroism, and size-exclusion chromatography. The three techniques produced coincident unfolding curves. Furthermore, the thermal unfolding seems also to be cooperative as the same temperature of half-denaturation is obtained using fluorescence and circular dichroism. Fld1−149 displays cold denaturation. The equilibrium properties of Fld1−149 demonstrate that molten globules lacking well-defined tertiary interactions can still be cooperatively stabilized and that cooperativity may appear in protein conformations of very low stability. This suggests that protein folding intermediates can, in principle, be cooperatively stabilized.

Many protein intermediate conformations, sharing properties of the folded and unfolded states, have been described in recent years. These intermediates are detected either when they accumulate transiently during refolding (*1*−*3*) or as the most stable conformations at equilibrium under certain conditions such as low pH (*4*, *5*), moderate concentrations of denaturant (*6*, *7*), or in mutant proteins where the native state is markedly destabilized (*8*, *9*). The intermediates are usually devoid of well-defined tertiary interactions (as indicated by their spectroscopic properties) but are still compact and often show high secondary structure contents. The term molten globule has been used to describe intermediate conformations of proteins where the secondary structure is formed but the more subtle tertiary interactions are absent (*10*). Molten globules have been proposed to be general intermediates in the folding pathway of many proteins (*11*) although some small proteins might escape this model (*12*, *13*). NMR[1] studies have allowed structural comparison of equilibrium molten globules with transient intermediates, and many similarities have been found (*14*−*16*). The study of the structure and energetics of protein intermediate conformations is of great importance to understand protein folding. In this context, one issue that is receiving much attention is whether protein intermediate conformations are cooperatively stabilized (*17*−*21*).

We are using the apoflavodoxin from *Anabæna* PCC 7119 as a model for folding and stability studies (*22*, *23*). Apoflavodoxin is a well-folded protein at pH 7.0 that forms an aggregated molten globule at low pH (*23*). Aiming at producing stable apoflavodoxin intermediates, we have destabilized the native conformation of apoflavodoxin by cleaving away its C-terminal helix. The resulting fragment (Fld1−149, Figure 1) is a monomer at pH 7.0, with spectroscopic and hydrodynamic properties of a molten globule. In this paper, we study the stability of this fragment to determine whether its structure is stabilized cooperatively by comparing the urea unfolding transitions measured by three different techniques (fluorescence, circular dichroism, and size-exclusion chromatography). We extend this analysis to thermal unfolding by comparing the temperatures of mid-denaturation measured by fluorescence and circular dichro-

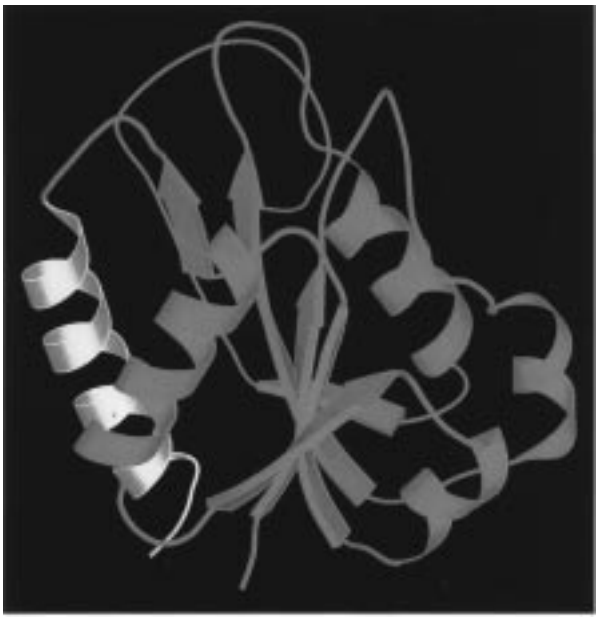

FIGURE 1: MOLSCRIPT representation (*34*) of uncleaved apoflavodoxin showing the sequence comprising amino acids 1−149 in orange and the C-terminal α-helix in white.

† We acknowledge financial support from the DGICYT (Grant PB94-0599, Spain). S.M. is a fellow of the Gobierno Vasco (Spain).

* Corresponding author. E-mail: jsancho@posta.unizar.es.

‡ Universidad de Zaragoza.

§ Instituto de Estructura de la Materia.

[1] Abbreviations: NMR, nuclear magnetic resonance; Fld1−149, flavodoxin fragment comprising residues 1−149; FPLC, fast-performance liquid chromatography; SDS−PAGE, sodium dodecyl sulfate−polyacrylamide gel electrophoresis; HPLC, high-performance liquid chromatography.

S0006-2960(98)00368-7 CCC: $15.00
Published on Web 07/03/1998

ism. A coincidence in unfolding curves measured by different techniques and including both chemical and thermal denaturation is expected for cooperatively stabilized folded conformations. On the other hand, the low conformational stability of Fld1−149 allows us to study if conformations of low stability can still be cooperative.

MATERIALS AND METHODS

Mutagenesis, Protein Cleavage, and Fragment Purification. Site-directed mutagenesis of the flavodoxin gene cloned in the plasmid pTrc99a (*24*) with a Y8C substitution was performed by the method of Deng and Nicholoff (*25*) using the oligonucleotide 5′TCTGTTAAGTCCATTTGATTATCTTC3′ to mutate the Ser149 wild-type codon to a methionine codon. Mutant plasmids were identified by direct sequencing. The mutant protein S149M was purified by a scaled-up adaptation of the method described for the wild-type protein (*24*). The mutant S149M contains only one methionine (the engineered one) and can thus be specifically cleaved at that position (*26*, *27*). S149M (2 mg/mL) was incubated for 24 h in 70% formic acid with 6.7 mg of cyanogen bromide/mg of protein, at room temperature in the dark. After incubation, most of the formic acid and cyanogen bromide were removed in vacuo at 25 °C. Then, 10 volumes of distilled water was added, and the solution was frozen and lyophilized. The lyophilized reaction mixture was dissolved in 50 mM Tris-HCl, pH 8, containing 5 M urea, and loaded onto an FPLC MonoQ HR 10/10 column from Pharmacia equilibrated in the same buffer. The N-terminal fragment, Fld1−149, was eluted from the column using a linear NaCl gradient (0−0.5 M in 48 min) in the same buffer. Further purification of Fld1−149 to eliminate traces of uncleaved protein was achieved using an FPLC Pro RPC 15 μM HR 10/10 column from Pharmacia using a linear gradient of acetonitrile (27−35% in 52 min) in 50 mM ammonium acetate, pH 5.5, containing 5 M urea. The fragment solution was dialyzed against 1 mM sodium phosphate, pH 7. The resulting Fld1−149 fragment was pure by SDS−PAGE and reverse-phase HPLC.

Absorbance, Fluorescence, Circular Dichroism, and ^{1}H NMR Spectra. The concentration of Fld1−149 was determined from the absorbance at 280 nm (*28*) using an extinction coefficient of 28 127 M^{-1} cm^{-1}. Absorbance spectra were recorded at 25.0 ± 0.1 °C in a Kontron Uvikon 860 spectrophotometer. Fluorescence emission spectra (excitation at 280 nm) were acquired at 25.0 ± 0.1 °C in a Kontron SMF 25 fluorometer. Circular dichroism spectra were recorded in a Jasco 710 spectropolarimeter: the far-UV spectra were recorded at 25 ± 2 °C using a 0.1 cm cuvette and the near-UV spectra at 25 ± 0.1 °C in a 1 cm cuvette. ^{1}H NMR spectra were acquired on a Bruker AMX-600 pulse spectrometer using 32K data points (zero-filled to 64K data points before performing the Fourier transformation). The temperature, calibrated with a methanol sample, was 25.0 ± 0.5 °C. Sodium 3-(trimethylsilyl)-[2,2,3,3-^{2}H]-propionate (TPS) was used as an internal reference.

Determination of Apparent Molecular Weight and Stokes Radius of Fld1−149. The apparent molecular weight and Stokes radius of Fld1−149 were determined by molecular exclusion chromatography using a fully automated FPLC (Pharmacia) with a Superose 12HR 10/30 column equilibrated in 50 mM sodium phosphate, pH 7, containing 0.5 M NaCl. The flow rate was 0.5 mL/min. The Stokes radius of Fld1−149 was determined from the molecular weight using the general equation proposed by Uversky (*29*).

Urea Denaturation. Denaturing samples of different urea concentrations were prepared in 5 mM sodium phosphate (with 0.5 M NaCl when indicated). Unfolding curves of Fld1−149 were obtained from the fluorescence emission (ratio of emission at 320 nm over 380 nm; excitation at 280 nm) and circular dichroism (222 nm) of the samples. An additional unfolding curve was obtained from the elution volumes of Fld1−149 samples loaded onto an FPLC Superose 12 HR 10/30 column from Pharmacia equilibrated in different urea concentrations. The data were analyzed, assuming a two-state equilibrium and a linear relationship between free energy and urea concentration (*30*), using the equation:

$$S = \frac{S_F + S_U e^{-(\Delta G_w - mD)/RT}}{1 + e^{-(\Delta G_w - mD)/RT}} \quad (1)$$

where S is the observed signal (either a spectroscopic property or an elution volume), S_F the signal of the folded state, S_U the signal of the unfolded state, ΔG_w the Gibbs energy difference between the folded and unfolded states in the absence of denaturant, D the concentration of denaturant (urea), and m the slope of the linear plot of ΔG versus D.

Thermal Denaturation. Unfolding was followed by fluorescence emission (ratio of emission at 350 nm over 380 nm; excitation at 280 nm) and by circular dichroism (222 nm). The temperature was increased from −5 to 90 °C at approximately 1 °C/min in a sealed cuvette. The temperature was controlled by circulating water with an antifreezing substance around the cuvette. A thermocouple immersed in the cuvette was used to monitor the temperature. The buffer was 5 mM sodium phosphate containing 0.5 M NaCl. The unfolding curves were analyzed as described (*30*) using the equation:

$$S = \frac{S_F + S_U e^{-(\Delta H(1-(T/T_m)) - \Delta C_p((T_m - T) + T\ln(T/T_m)))/RT}}{1 + e^{-(\Delta H(1-(T/T_m)) - \Delta C_p((T_m - T) + T\ln(T/T_m)))/RT}} \quad (2)$$

where T_m is the transition temperature, ΔH and ΔC_p are the enthalpy and specific heat of denaturation at T_m, respectively, and the other terms have the same meaning as in eq 1.

RESULTS AND DISCUSSION

Fld1−149 Is a Monomeric Molten Globule. Highly purified (>99%) Fld1−149 was recovered after purification as judged by SDS−PAGE (Figure 2) and reverse-phase HPLC (not shown). Mass spectroscopy analysis (MALDI, not shown) of Fld1−149 showed a single peak centered at 16 472 ± 3 Da (mean of three determinations ± SD), in good agreement with the theoretical mass (16 468). Since removal of the C-terminal helix was expected to significantly destabilize apoflavodoxin, we first studied whether the resulting fragment was nativelike, a molten globule, or simply denatured.

The helical content of the fragment (calculated from the ellipticity at 222 nm, Figure 3A) can be compared to that of the uncleaved protein. According to our calculation, the

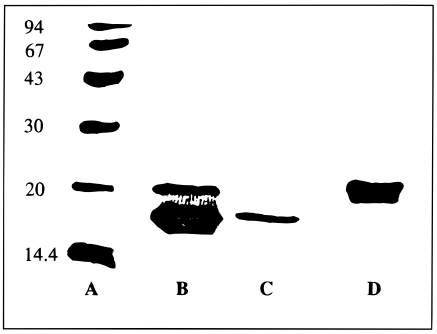

FIGURE 2: SDS−PAGE of apoflavodoxin and the Fld1−149 fragment: (A) molecular weight markers; (B) cleavage mixture after 24 h; (C) purified Fld1−149; (D) uncleaved apoflavodoxin.

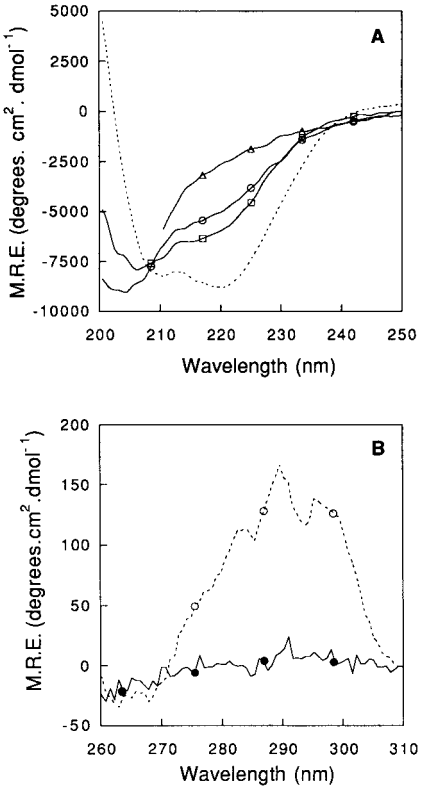

FIGURE 3: Circular dichroism spectra of Fld1−149 and uncleaved apoflavodoxin. (A) Far-UV spectra: (open circles) Fld1−149 in 5 mM sodium phosphate, pH 7.0; (open triangles) Fld1−149 in 5 mM sodium phosphate, pH 7.0, with 5 M urea; (open squares) Fld1−149 in 5 mM sodium phosphate, pH 7.0, with 0.5 M NaCl; (dashed line) uncleaved apoflavodoxin (S149M) in 5 mM sodium phosphate, pH 7.0, with 0.5 M NaCl. (B) Near-UV spectra: (solid circles) Fld1−149 in 5 mM sodium phosphate, pH 7.0, with 0.5 M NaCl; (open circles) uncleaved apoflavodoxin (S149M) in the same buffer.

helical content of the fragment represents around 65% of the helical content of the corresponding segment of the uncleaved protein (after subtraction of the contribution of the C-terminal helix that is not present in the fragment). Further, the helical content of Fld1−149 is increased to around 80% of the content displayed in the uncleaved protein (Figure 3A) by addition of 0.5 M NaCl. This enhancement of the helical content is not exerted by an equivalent concentration of choline chloride (not shown) and seems to be related to sodium binding (see Discussion). A similar sodium-related stabilization effect is observed in the uncleaved protein (unpublished results). In 5 M urea, the Fld1−149 helical content is very low (Figure 3A). Since NaCl enhances the helical content of Fld1−149, we have used this salt at a 0.5 M concentration throughout this study. Most of the observations reported for the fragment in the presence of 0.5 M NaCl are also qualitatively valid for the fragment in the absence of NaCl (not shown).

Although, in 0.5 M NaCl, the helical contents of Fld1−149 and the corresponding segment of uncleaved apoflavodoxin are similar, the near-UV circular dichroism spectra of Fld1−149 and uncleaved apoflavodoxin are very different (Figure 3B). While the uncleaved apoprotein displays a well-defined spectrum with several distinct peaks, the spectrum of the fragment is flat regardless of the presence of 0.5 M NaCl. This is an indication of a lack of stable tertiary interactions involving aromatic amino acids in the fragment, but since the fragment lacks one of the four tryptophan residues that are present in the uncleaved protein, additional proof of a molten globule character is required.

A lack of well-defined tertiary interactions in Fld1−149 is confirmed by the comparison of 1D ^{1}H NMR spectra of Fld1−149 and uncleaved protein in 0.5 M NaCl in water presented in Figure 4. In contrast with the uncleaved protein (A), no Fld1−149 high-field signals are observed (B), and the aromatic protons of the fragment are clustered in the random coil region. Further, the large dispersion of the amide protons in the uncleaved protein (A) is drastically reduced in the fragment (B). In contrast with the uncleaved protein, the amide protons of Fld1−149 exchange completely within a few minutes after a lyophilized sample is dissolved in D_2O (data not shown). The broad signals of the Fld1−149 spectrum are characteristic of molten globule states (*20*). To rule out the possibility that the observed line broadening is due to aggregation, we have recorded ^{1}H NMR spectra in D_2O at two different fragment concentrations (0.1 mM and 1 mM). The two spectra (Figure 5A,B) have identical line widths and chemical shifts. Sharp peaks appear, as expected, in the spectrum of the fragment denatured in urea (Figure 5C). The circular dichroism and NMR data together indicate thus that Fld1−149 combines a high helical content with the lack of tertiary interactions that characterizes molten globules.

Molten globules must also be compact. Compaction of a polypeptide chain often leads to the burial of tryptophan residues with a concomitant blue shift of the fluorescence emission and absorbance maxima. Fld1−149 contains three tryptophan residues and has an emission maximum in 0.5 M NaCl at 340 nm (Figure 6). This is close to the maximum of the uncleaved protein (with four tryptophan residues) at 335 nm. The emission maximum in the fragment is sensitive to solvent conditions: in the absence of NaCl, it moves to 350 nm, and in the presence of 5 M urea, it moves to 355 nm, which is typical of unfolded proteins. Thus, some of the tryptophan residues of Fld1−149 in 0.5 M NaCl seem to be shielded from solvent, indicating the presence of a compact conformation. This evidence is supported by the absorbance difference spectra of the fragment (similar in shape to that of the uncleaved protein; Figure 7) that are typical of conformations with buried tryptophan residues (*31*).

Size-exclusion chromatography provides additional proof of compaction. Fld1−149 is eluted from a gel filtration column as a single peak whose elution volume is concentra-

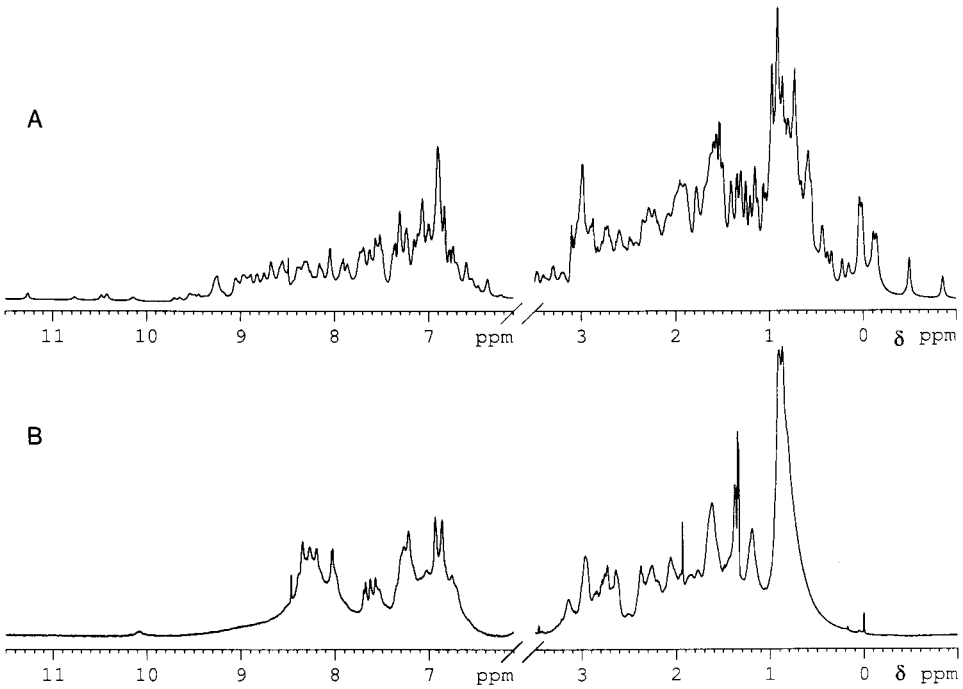

FIGURE 4: Selected regions of the 1D ^{1}H NMR spectra of uncleaved apoflavodoxin in water [(A) 2 mM apoflavodoxin in 20 mM sodium phosphate, pH 7.0, 0.5 M NaCl, 2 mM DTT, and H_2O/D_2O (9:1) at 25 ± 0.5 °C] and Fld1−149 [(B) 1 mM Fld1−149 in 20 mM sodium phosphate, pH 7.0, 0.5 M NaCl, 1 mM DTT, and H_2O/D_2O (9:1) at 25 ± 0.5 °C].

tion-independent from 0.3 to 2.4 μM (not shown). In 50 mM sodium phosphate and 0.5 M NaCl, pH 7.0, the apparent molecular weight of the fragment is 21.0 kDa. However, since the fragment is not fully folded, this apparent molecular mass is an overestimate. When the gel filtration urea unfolding curve is fitted to eq 1 (data not shown), the elution volume of fully folded Fld1−149 can be calculated, and from this volume, the apparent molecular weight of fully folded Fld1−149 is estimated at 19.1 kDa. The apparent molecular mass for the uncleaved protein in the same conditions is 21.5 kDa (the same value is calculated from the fitted elution volume of fully folded protein since the protein is fully folded under these conditions). The determined molecular masses for the fragment and the uncleaved protein are close to the actual ones (16.6 and 18.8 kDa, respectively), indicating that the fragment is monomeric. The Stokes radii for the folded fragment and protein are 22.9 and 24.3 Å, respectively, suggesting a similar compaction. The Stokes radius of the fragment in 5 M urea (37.7 Å) indicates that it is fully unfolded by urea (*29*).

Size-exclusion chromatography thus confirms the spectroscopic evidence indicating that Fld1−149 is in a compact conformation. The calculated molecular mass and the independence of the elution volume on fragment concentration indicate that Fld1−149 is a monomer, at least up to 2.4 μM. Evidence of a monomeric conformation of Fld1−149 at higher concentrations is supported by the independence of the conformational stability on concentration from 0.8 to 8.0 μM and from 2 to 20 μM (see Tables 1 and 2) and by the lack of effects in line widths and chemical shifts in NMR spectra from 0.1 to 1.0 mM (Figure 5).

Fld1−149 is thus a monomeric molten globule, the stability of which can be conveniently analyzed by conventional procedures without the complications arising from aggregated molten globules.

Fld1−149 Is Cooperatively Stabilized. A critical test to examine if a protein conformation is cooperatively stabilized is the superposition of the unfolding curves monitored using different techniques. This test has been applied to the apomyoglobin pH 4 intermediate whose fluorescence and circular dichroism curves are superimposable with the exception of the more unstable mutants (*21*). We have used this approach to study the cooperativity of Fld1−149 by comparing the urea unfolding curves monitored by three different techniques, fluorescence, circular dichroism, and size-exclusion chromatography, and by comparing the temperature of mid-denaturation obtained by two different techniques: fluorescence and circular dichroism.

Fld1−149 can be unfolded by moderate concentrations of urea (Figure 8), and the unfolding is reversible (not shown). The fluorescence and circular dichroism curves are similar and can be fitted to a two-state transition (eq 1). The calculated values of ΔG are the same (around −1.1 kcal mol^{-1}) for both techniques and do not change with fragment concentration from 0.8 to 8 μM (Table 1). The slope of the transition (m in eq 1) is also the same for both techniques (around 0.8 kcal mol^{-1} M^{-1}), and no concentration dependence is observed (Table 1). The urea concentration of mid-denaturation is around 1.5 M in all cases. This coincidence of the fluorescence and circular dichroism unfolding curves is already a strong indication that Fld1−149 is cooperatively stabilized. Nevertheless, size-exclusion chromatography has also been applied to study the unfolding. Fitting of the size-exclusion unfolding curve to eq 1 gives an m value of 0.73 ± 0.06 kcal mol^{-1} M^{-1}, which is in agreement with m values obtained previously. However, the midpoint transition occurs at 1.98 ± 0.06 M urea, and the calculated value of ΔG is 1.45 ± 0.14 kcal mol^{-1}. The molecular exclusion unfolding curve gives a value of $[\text{urea}]_{1/2}$ which is rather different from those obtained using fluores-

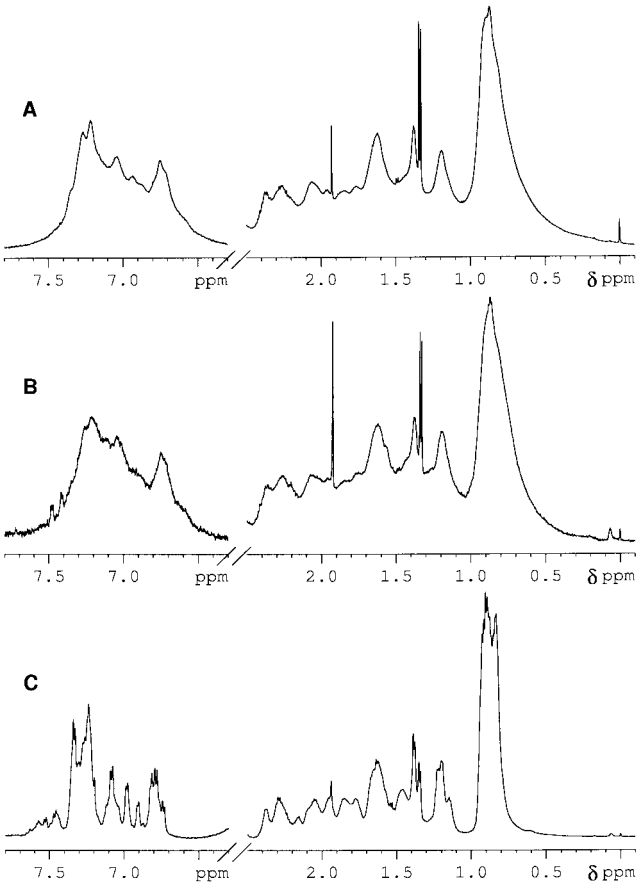

FIGURE 5: Aromatic and aliphatic regions of the 1D ^{1}H NMR spectra of Fld1−149 in D_2O at 25 ± 0.5 °C: (A) 1 mM Fld1−149 in 20 mM sodium phosphate, pH 7.0, 0.5 M NaCl, and 1 mM DTT; (B) 0.1 mM Fld1−149 in the same conditions (except 0.1 mM DTT); (C) 1 mM Fld1−149 in 20 mM sodium phosphate, pH 7.0, 4 M urea, 0.5 M NaCl, and 1 mM DTT.

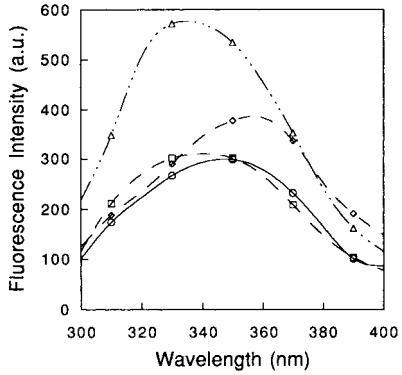

FIGURE 6: Fluorescence spectra of Fld1−149 and uncleaved apoflavodoxin (S149M): (open circles) Fld1−149 in 5 mM sodium phosphate, pH 7.0; (open squares) Fld1−149 in 5 mM sodium phosphate, pH 7.0, with 0.5 M NaCl; (open diamonds) Fld1−149 in 5 mM sodium phosphate, pH 7.0, with 5 M urea; (open triangles) uncleaved apoflavodoxin (S149M) in 5 mM sodium phosphate, pH 7.0, with 0.5 M NaCl.

cence and circular dichroism. According to Uversky (*29*), the Superose 12HR 10/30 column from Pharmacia does not alter the equilibrium between folded and unfolded proteins. If this is indeed the case, the difference between the determined values of urea concentration at mid-denaturation would imply that an intermediate accumulates at equilibrium in the unfolding region. But for the uncleaved protein [whose unfolding equilibrium is two-state (*23*)], we have

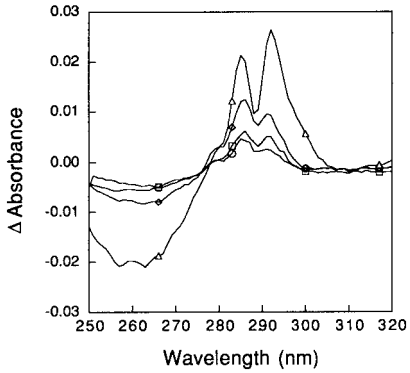

FIGURE 7: Near-UV absorbance difference spectra of Fld1−149 and uncleaved apoflavodoxin (S149M). All spectra recorded in 5 mM sodium phosphate, pH 7.0, plus either 4 M urea or 0.5 M NaCl (as indicated). Spectra: (open circles) Fld1−149 with minus without NaCl; (open squares) Fld1−149 without minus with urea; (open diamonds) Fld1−149 with NaCl minus with urea; (open triangles) uncleaved apoflavodoxin (S149M) with NaCl minus with urea.

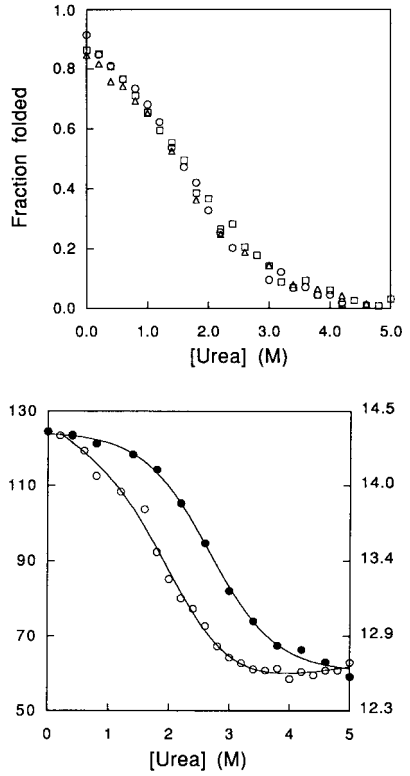

FIGURE 8: (Top) Fraction of folded Fld1−149 as a function of urea concentration: (open circles) fluorescence; (open squares) circular dichroism; (open triangles) size-exclusion chromatography. The data have been fitted to eq 1 to obtain the fraction folded as a function of urea concentration. The effect of the Superose 12HR 10/30 column on the observed stability of Fld1−149 has been subtracted assuming that it is the same as the effect observed for the uncleaved protein (see Results and bottom panel). (Bottom) Effect of the Superose 12HR 10/30 column on the observed stability of uncleaved S149M in 5 mM sodium phosphate, pH 7.0, with 0.5 M NaCl: (open circles) urea unfolding curve followed by fluorescence; (closed circles) urea unfolding curve followed by size-exclusion chromatography. The fluorescence curve of the uncleaved protein was fitted using the Santoro−Bolen correction (*35*) of eq 1 as described for wild-type apoflavodoxin (*23*).

observed that the urea concentration required to denature half of the protein molecules is 0.45 M unit higher when it is measured by size-exclusion chromatography using the column than when it is measured spectroscopically (bottom

Table 1: Urea Denaturation of Fld1−149 by Different Techniques[a]

	fluorescence	circular dichroism	size-exclusion chromatography
ΔG (kcal mol^{-1})	-1.24 ± 0.24[b]	-1.05 ± 0.12[b]	-1.12 ± 0.06[d]
	-1.15 ± 0.23[c]	-1.13 ± 0.11[c]	
m (kcal mol^{-1} M^{-1})	0.85 ± 0.11[b]	0.68 ± 0.05[b]	0.73 ± 0.06[d]
	0.75 ± 0.09[c]	0.85 ± 0.11[c]	
$U_{1/2}$ (M)	1.46 ± 0.12[b]	1.55 ± 0.07[b]	1.53 ± 0.06[d]
	1.52 ± 0.13[c]	1.52 ± 0.07[c]	

[a] At 25.0 ± 0.1 °C in 5 mM sodium phosphate with 0.5 M NaCl. Errors provided by the fitting program. The size-exclusion data were acquired at 25 ± 2 °C. [b] 0.8 μM Fld1−149. [c] 8.0 μM Fld1−149. [d] 1.2 μM Fld1−149. The urea concentration of half-denaturation has been corrected as explained in the Results section. The stability is calculated from the corrected half urea and the observed m value.

panel in Figure 8), although the transition slope does not change significantly. This suggests that interactions between the protein and the column stabilize the folded conformation. Assuming a similar effect for the Fld1−149 fragment, the apparent half urea measured by size-exclusion chromatography must be corrected by subtracting 0.45 M unit. This gives a final value of 1.53 M, which coincides with the values determined by fluorescence and circular dichroism measurements (Table 1 and Figure 8). Since the observed slope of the transition in the size-exclusion unfolding is the same as those of the spectroscopically monitored unfolding, the corrected size-exclusion unfolding curve coincides with the spectroscopically determined curves and the same stability is calculated (Figure 8 and Table 1). The fact that three different techniques report the same stability for the fragment (and the same slope m) strongly indicates that the urea unfolding is a cooperative process where only two states are populated.

The cooperative stabilization of Fld1−149 can be further probed by applying the superposition test to the thermal unfolding. For the thermal unfolding monitored by fluorescence we have plotted the ratio of fluorescence emission at two different wavelengths versus temperature (Figure 9A). This minimizes the strong effect of temperature on fluorescence that often causes important distortions. In this way a simple sigmoidal unfolding curve that can be fitted to a two-state model (eq 2) is obtained. When eq 2 is used $\Delta H(T_m)$, ΔC_p and T_m values are obtained, but the error in ΔC_p is usually large (*30*), and therefore only $\Delta H(T_m)$ and T_m are accepted as meaningful values. Using 2 μM Fld1−149 the transition temperature is $T_m = 46.0 \pm 2.5$ °C (mean of three experiments ± SD; Table 2) and $\Delta H(T_m)$ is -12.3 ± 0.6 kcal mol^{-1} (mean of three experiments ± SD). Similar results [T_m = 46.7 °C and $\Delta H(T_m) = -12.9$ kcal mol^{-1}] were obtained with a 20 μM Fld1−149 solution (Table 2).

When the thermal unfolding is followed by circular dichroism, the signal becomes less negative at both low and high temperatures, indicating that the fragment experiences both heat and cold denaturation (Figure 10). The entire unfolding curve (from −5 to +90 °C) was fitted to eq 2, and the fitted values obtained were $T_m = 48.3 \pm 1.3$ °C (mean of three experiments ± SD; Table 2), $\Delta H(T_m) = -17.0 \pm 1.8$ kcal mol^{-1}, and $\Delta C_p = 0.73 \pm 0.05$ kcal mol^{-1} K^{-1}. Enthalpy values calculated using eq 2 are usually less accurate than transition temperatures, and the reported difference in enthalpy values between fluorescence and circular dichroism data may not be significant. Importantly,

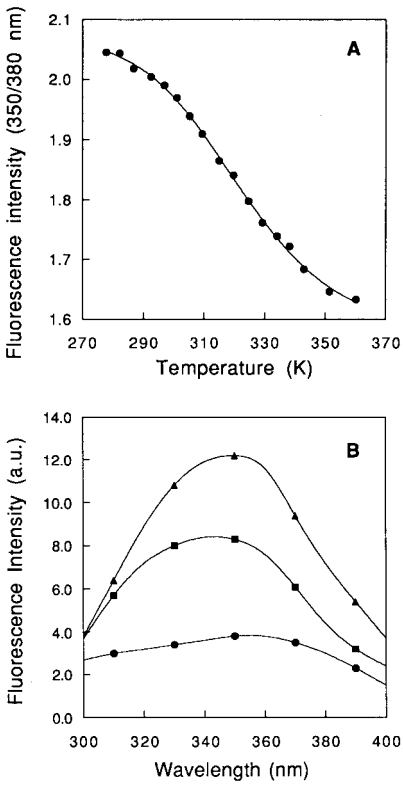

FIGURE 9: Thermal denaturation of Fld1−149 followed by fluorescence. All samples were in 5 mM sodium phosphate, pH 7.0, with 0.5 M NaCl. (A) Unfolding curve (ratio of intensities 350/380 nm). The solid line is the fitting of the data to eq 2. (B) Fluorescence spectra of Fld1−149 at different temperatures: (closed triangles) 3 °C; (closed squares) 27 °C; (closed circles) 68 °C.

Table 2: Thermal Denaturation of Fld1−149 by Different Techniques[a]

	fluorescence	circular dichroism
T_m (°C)	46.0 ± 2.5[b]	48.3 ± 1.3[b]
	46.7[c]	
ΔH (kcal mol^{-1})	12.3 ± 0.6[b]	17.0 ± 1.8[b]
	12.9[c]	
ΔC_p (kcal mol^{-1} K^{-1})	unreliable	0.73 ± 0.05[b]

[a] In 5 mM sodium phosphate with 0.5 M NaCl. Errors are the standard deviations of three experiments. [b] 2.0 μM Fld1−149. [c] 20.0 μM Fld1−149.

the same transition temperature is obtained for fluorescence and circular dichroism-monitored unfolding curves. This indicates that, as in the case of urea denaturation, the thermal unfolding of Fld1−149 is cooperative and consistent with a two-state mechanism. Fld1−149 thus passes the superposition test in both urea and thermal unfolding.

Fld1−149 Experiences Cold Denaturation. The circular dichroism thermal unfolding curve (Figure 10) shows that Fld1−149 becomes destabilized at both high and low temperatures. At the temperature of highest helical content (27 °C) the ellipticity is around 90% of the maximal calculated ellipticity (Θ_F in eq 2). The fluorescence unfolding curve (I_{350}/I_{380} versus temperature, Figure 9A) does not show an equivalent change at low temperature, suggesting that the ratios of intensities are similar in the folded and cold-denatured conformations of Fld1−149. Notwithstanding, the cold denaturation of Fld1−149 can be observed by fluorescence from the change in the position of the emission maximum at different temperatures. At 27 °C the maximum

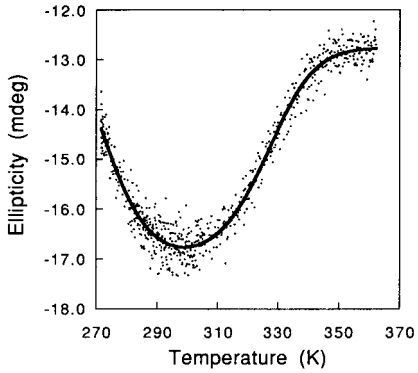

FIGURE 10: Thermal denaturation of Fld1−149 followed by circular dichroism (222 nm). The sample was in 5 mM sodium phosphate, pH 7.0, with 0.5 M NaCl. The solid line is the fitting of the data to eq 2.

is at 340 nm (Figure 9B). At high temperature (68 °C), where denaturation is almost complete, the maximum is at 353 nm, and at 3 °C, close to the temperature of cold denaturation, the maximum of fluorescence emission is at 348 nm.

Cold denaturation is favored by a large ΔC_p and a small ΔH of unfolding (*32*, *33*). The thermal denaturation of wild-type uncleaved flavodoxin has been studied in detail by calorimetry (*23*). The heat capacity and enthalpy of denaturation (at T_m) for this protein at pH 7.0 are 1.36 kcal mol^{-1} K^{-1} and 63.3 kcal mol^{-1}, respectively. The uncleaved wild-type protein has maximal stability at 24 °C and the cold denaturation temperature is well below zero. In the Fld1−149 fragment, the lower enthalpy of denaturation (−12−17 kcal mol^{-1} at T_m) favors a higher cold denaturation temperature of 7 °C (see ref *32* for details on the calculation). Cold denaturation of proteins requires a positive and significant heat capacity of unfolding. The direct measurement by calorimetry of the Fld1−149 ΔC_p was attempted, but the transition could not be observed (Dr. M. Cortijo and Dr. D. Remeta, personal communications), probably because it is too broad. Another way to estimate the value of ΔC_p for Fld1−149 is from the fitting of the spectroscopically observed thermal transitions to eq 2. Determination of reliable values of ΔC_p from a fitting to eq 2 of simple heat denaturation curves (such as the fluorescence curve in Figure 9A) requires exceptionally good experimental data (*30*), and for this reason, we do not trust the ΔC_p value derived from the fitting of the fluorescence unfolding curve (value not reported). However, the circular dichroism denaturation curve (Figure 10) is different because both heat and cold denaturation are evident. Since the curvature of the data at low temperature is a ΔC_p-linked effect, the value of ΔC_p derived from the fitting to eq 2 is reliable. This value is $\Delta C_p = 0.73 \pm 0.05$ kcal mol^{-1} K^{-1} (mean of three experiments ± SD). The fragment Fld1−149 thus fulfills the conditions of having a small enthalpy of denaturation and yet a significant and positive heat capacity, which set the transition temperature of cold denaturation above zero.

Comparison with the Uncleaved Protein. Wild-type apoflavodoxin is a well-folded protein of low conformational stability (*22*, *23*). At low pH apoflavodoxin is in a molten globule-like conformation whose stability can be determined by urea denaturation (*23*). Unfortunately, at low pH apoflavodoxin is aggregated, and therefore any stability measurement reports on both the stability of the monomer and that of the aggregation equilibrium. Destabilization of apoflavodoxin by cleaving the C-terminal helix leads to the Fld1−149 fragment that is a monomeric molten globule at pH 7.0 (see above). The stability of this molten globule, which can be determined without complications arising from aggregation, is very low: in the presence of 0.5 M NaCl only 90% of the molecules are folded. The effect of NaCl on the stability of Fld1−149 is not exerted by the bulky cation-containing choline chloride, which suggests that it is a cation binding effect rather than an ionic strength effect. The same NaCl effect on the stability of the uncleaved protein has been observed (unpublished) that probably reflects the presence of sodium binding sites in the protein. The persistence of the sodium effect in the fragment suggests that the putative sodium binding sites are also present in it, and this in turn suggests that the fold of the fragment might not be very different from that of the uncleaved protein. Size-exclusion chromatography indicates that Fld1−149 is not significantly less compact than uncleaved apoflavodoxin. In Fld1−149, however, the hydrophobic side chains are more exposed to solvent than in the uncleaved protein, as indicated by the lower *m* values in equilibrium urea denaturation and the lower ΔC_p of unfolding. This may indicate that the hydrophobic core is partly hydrated or may simply reflect the exposure of hydrophobic surface as a consequence of the removal of the C-terminal helix.

Conclusions. The most interesting finding of this study is that the Fld1−149 fragment is stabilized cooperatively (as it is uncleaved apoflavodoxin) since urea denaturation unfolding curves yield the same thermodynamic parameters regardless of technique, and the same applies to thermal unfolding. This is positive evidence that molten globules, lacking well-defined tertiary interactions, can be cooperatively stabilized and that cooperativity is not a qualitative criterion that separates well-folded proteins from less ordered intermediates. Previous studies on the apomyoglobin pH 4 intermediate (*21*) have related the persistence of cooperativity with a sufficiently high stability of the compact conformation. Our studies on Fld1−149 indicate that cooperative stabilization can occur when the conformational stability is as low as 1 kcal mol^{-1}. If this can be extrapolated to other proteins, it means that cooperativity is potentially within the reach of any major folding intermediate.

ACKNOWLEDGMENT

We thank E. González for her involvement in an early stage of this work and A. Lostao for preparing the S149M mutant.

REFERENCES

1. Roder, H., Elove, G. A., and Englander, S. W. (1988) Structural characterization of folding intermediates in cytochrome *c* by H-exchange labeling and proton NMR, *Nature 335*, 700−704.
2. Udgaonkar, J. B., and Baldwin, R. L. (1988) Evidence for an early folding intermediate on the folding pathway of ribonuclease A, *Nature 335*, 694−699.
3. Matouschek, A., Kellis, J. T., Jr., Serrano, L., Bycroft, M., and Fersht, A. R. (1990) Transient folding intermediates characterized by protein engineering, *Nature 346*, 440−445.
4. Griko, Yu., Privalov, P. L., Venyaminov, S. Yu., and Kutyshenko, V. P. (1988) Thermodynamic study of the apomyoglobin structure, *J. Mol. Biol. 202*, 127−138.

5. Bychkova, E. V., Berni, R., Rossi, G. L., Kutyshenko, V. P., and Ptitsyn, O. B. (1992) Retinol-binding protein is in the molten globule state at low pH, *Biochemistry 31*, 7566−7571.
6. Kuwajima, K., Nitta, K., Yoneyama, M., and Sugai, S. (1976) Three-state denaturation of alpha-lactalbumin by guanidine hydrochloride, *J. Mol. Biol. 106*, 359−373.
7. Robson, B., and Pain, R. H. (1976) The mechanism of folding of globular proteins. Equilibria and kinetics of conformational transitions of penicillinase from *Staphylococcus aureus* involving a state of intermediate conformation, *Biochem. J. 155*, 331−344.
8. Shortle, D., and Meeker, A. K. (1989) Residual structure in large fragments of staphylococcal nuclease: effects of amino acid substitutions, *Biochemistry 28*, 936−944.
9. Lim, W. A., Farruggio, D. C., and Sauer, R. T. (1992) Structural and energetic consequences of disruptive mutations in a protein core, *Biochemistry 31*, 4324−4333.
10. Ohgushi, M., and Wada, A. (1983) "Molten-globule state": a compact form of globular proteins with mobile side-chains, *FEBS Lett. 164*, 21−24.
11. Ptitsyn, O. B. (1992) The molten globule state, in *Protein Folding* (Creighton, T. E., Ed.) pp 243−300, Freeman, New York.
12. Jackson, S. E., and Fersht, A. R. (1991) Folding of chymotrypsin inhibitor 2. 1. Evidence for a two-state transition, *Biochemistry 30*, 10428−10435.
13. Alexander, P., Orban, J., and Bryan, P. (1992) Kinetic analysis of folding and unfolding the 56-amino acid IgG binding domain of streptococcal protein-G, *Biochemistry 31*, 7243−7248.
14. Jennings, P. A., and Wright, P. E. (1993) Formation of a molten globule intermediate early in the kinetic folding pathway of apomyoglobin, *Science 262*, 892−896.
15. Balbach, J., Forge, V., van Nuland, N. A. J., Winder, S. L., Hore, P. J., and Dobson, C. M. (1995) Following protein folding in real time using NMR spectroscopy, *Nat. Struct. Biol. 2*, 866−870.
16. Raschke, T. M., and Marqusee, S. (1997) The kinetic folding intermediate of ribonuclease H resembles the acid molten globule and partially unfolded molecules detected under native conditions, *Nat. Struct. Biol. 4*, 298−304.
17. Schulman, B. A., and Kim, P. S. (1996) Proline scanning mutagenesis of a molten globule reveals noncooperative formation of protein′s overall topology, *Nat. Struct. Biol. 3*, 682−687.
18. Jamin, M., and Baldwin, R. L. (1996) Refolding and unfolding kinetics of the equilibrium folding intermediate of apomyoglobin, *Nat. Struct. Biol. 3*, 613−618.
19. Kay, M. S., and Baldwin, R. L. (1996) Packing interactions in the apomyoglobin folding intermediate, *Nat. Struct. Biol. 3*, 429−445.
20. Schulman, B. A., Kim, P. S., Dobson, C. M., and Redfield, C. (1997) A residue-specific NMR view of the noncooperative unfolding of a molten globule, *Nat. Struct. Biol. 4*, 630−634.
21. Luo, Y., Kay, M. S., and Baldwin, R. L. (1997) Cooperativity of folding of the apomyoglobin pH 4 intermediate studied by glycine and proline mutations, *Nat. Struct. Biol. 4*, 925−930.
22. Genzor, C. G., Perales-Alcón, A., Sancho, J., and Romero, A. (1996) Closure of a tyrosine/tryptophane aromatic gate leads to a compact fold in apoflavodoxin, *Nat. Struct. Biol. 3*, 329−332.
23. Genzor, C. G., Beldarraín, A., Gómez-Moreno, C., López-Lacomba, J. L., Cortijo, M., and Sancho, J. (1996) Conformational stability of apoflavodoxin, *Protein Sci. 5*, 1373−1388.
24. Fillat, M. F., Borrias, W. E., and Weisbeerk, PJ. (1991) Isolation and overexpression in *Escherichia coli* of the flavodoxin gene from *Anabæna* PCC 7119, *Biochem. J. 280*, 187−191.
25. Deng, W. P., and Nickoloff, J. A. (1992) Site-directed mutagenesis of virtually any plasmid by eliminating a unique site, *Anal. Biochem. 200*, 81−88.
26. Gross, E., and Witkop, B. J. (1961) Selective cleavage of the methionyl peptide bonds in ribonuclease with cyanogen bromide, *J. Am. Chem. Soc. 83*, 1510−1511.
27. Sancho, J., and Fersht, A. R. (1992) Dissection of an enzyme by protein engineering. The N- and C-terminal fragments of barnase form a nativelike complex with restored enzymic activity, *J. Mol. Biol. 224*, 741−747.
28. Gill, S. C., and von Hippel, P. H. (1989) Calculation of protein extinction coefficients from amino acid sequence data, *Anal. Biochem. 182*, 319−326.
29. Uversky, V. N. (1993) Use of fast protein size-exclusion chromatography to study the unfolding of proteins that denature though the molten globule, *Biochemistry 32*, 13288−13298.
30. Pace, C. N., Shirley, B. A., and Thomson, J. A. (1989) Measuring the conformational stability of a protein, in *Protein structure, a practical approach*, pp 311−330, IRL Press, Oxford.
31. Schmid, F. X. (1989) Spectral methods of characterizing protein conformation and conformational changes, in *Protein structure, a practical approach*, pp 251−285, IRL Press, Oxford.
32. Privalov, P. L. (1990) Cold denaturation of proteins, *Crit. Rev. Biochem. Mol. Biol. 25*, 281−305.
33. Nishii, I., Kataoka, M., Tokunaga, F., and Goto, Y. (1994) Cold denaturation of the molten globule states of apomyoglobin and a profile for protein folding, *Biochemistry 33*, 4903−4909.
34. Kraulis, P. J. (1991) MOLSCRIPT: a program to produce both detailed and schematic plots of protein structures, *J. Appl. Crystallogr. 24*, 946−950.
35. Santoro, M. M., and Bolen, D. W. (1988) Unfolding free-energy changes determined by the linear extrapolation method. 1. Unfolding of phenylmethanesulfonyl alpha-chymotrypsin using different denaturants, *Biochemistry 27*, 8063−8068.

BI980368X